Landslides caught on seismic networks and satellite radars

Andrea Manconi[1]*, Alessandro C. Mondini[2], and the ALPARRAY Working Group

[1]Department of Earth Sciences, Engineering Geology, ETH Zurich, Switzerland

[2]National Research Council, Istituto di Ricerca per la Protezione Idrogeologica, Perugia, Italy

Corresponding author: first and last name (andrea.manconi@erdw.ethz.ch)

Key Points:

- Seismic data and satellite radar imagery are jointly used to detect and characterize landslides
- The method is validated on a recent sequence of landslides in the Swiss Alps
- The operational implementation of our approach can be used to improve the completeness of landslide catalogues

Abstract

We present a procedure to detect landslide events by jointly analyzing data acquired from regional broadband seismic networks and spaceborne radar imagery. To validate the method, we consider a series of six slope failures associated to the Piz Cengalo rock avalanche recently occurred in the Swiss Alps, a region where we can benefit from high spatial density and quality of seismic data, as well as from the high spatial and temporal resolution of the ESA Copernicus Sentinel-1 radar satellites. The operational implementation of the proposed approach, in combination with the future increase in availability of seismic and satellite data, can offer a new and efficient solution to build and/or expand landslide catalogues based on quantitative measurements, which are the base of hazard assessment and early warning systems at regional scale.

Plain Language Summary

Information on when, where and how landslides events occur is the key to build complete catalogues and perform accurate hazard assessments. Despite recent efforts, quantitative datasets are rare. Here we show a procedure that allows to benefit from the increased density of seismic sensors installed on ground for earthquake monitoring, as well as from the unprecedented availability of satellite radar data. We show how the procedure works on a recent sequence of landslide occurred at Piz Cengalo (Swiss Alps) in 2017. The results show that our approach provide important information on the location and magnitude of landslide events, and could be used operationally to build more complete catalogues and eventually improve the accuracy of landslide hazard assessment.

1 Introduction

Landslides cause globally fatalities and devastation, with remarkable effects on low-income and/or developing countries (Froude & Petley, 2018). While the spatial occurrence of landslides is related to intrinsic geo-morphological, and climatic characteristics (Stead & Wolter, 2015), catastrophic failures arise when slope materials reach a critical damage state (Petley, 2004). In many cases, the ultimate trigger towards failure events is related to anthropic activities, extreme meteorological events, and earthquakes (Bayer et al., 2018; Huang Mong-Han et al., 2017; Lacroix et al., 2019).

Quantitative and accurate data on timing, location and size of landslides events are crucial to study the relationships between local and regional preconditioning factors, to recognize potential causes, as well as to identify the potential effects of climatic forcing. Moreover, efficient early warning systems at regional scale rely on the availability of accurate and complete landslide catalogues (Gariano & Guzzetti, 2016). Despite recent efforts, the knowledge on spatial and temporal landslide distribution is often incomplete. The information about landslide volume, runout, velocity, etc. is usually available only when the events threat life or damage infrastructures, as well as when they are associated with large earthquakes or exceptional meteorological occurrences. These catalogues, however, deliver only a partial picture of the impact of such events on the landscape. In addition, many landslide events are unreported because they occur in remote regions and do not have immediate and/or relevant impacts on human activities. This strongly hinders the completeness of inventories used for hazard assessment and for calibration of early warning systems at regional scales (Guzzetti et al., 2019).

In recent years, two methods dominated the panorama of landslide event detection, i.e. satellite remote sensing and seismic data analyses. This is mainly due to the increased availability and quality of these datasets at global scale, as well as to the open data access policies. In particular, Earth Observation (EO) data acquired through different satellite missions are more and more exploited by systematic visual interpretation, as well as supervised and unsupervised automatic classification methodologies, in order to build catalogues of landslide events triggered by large earthquakes and/or extreme meteorological events (Mondini et al., 2019; Tanyaş et al., 2017). Further, despite the identification of signatures of landslide events in seismic networks deployed for earthquake monitoring is not a new observation (Govi et al., 2002; Weichert et al., 1994), advances and diffusion of broadband seismic sensors have increased the possibility to detect and locate also landslide events of small-moderate size at regional scales. Automatic or semi-automatic procedures adapted from earthquake location routines have demonstrated good performances (Chao et al., 2017; Dammeier et al., 2011; Ekstrom, 2006; Fuchs et al., 2018); however, while uncertainties of several km can be tolerated in case of earthquake epicentral locations, landslides are extremely confined phenomena affecting a single slope (or only small portions of it). For this reason, a more accurate location of the events is necessary.

In this work, we jointly use broadband seismic data and spaceborne radar imagery to show a procedure allowing for a systematic detection and location of landslides, as well as an initial definition of their area of impact, and their magnitude. We present results over the region recently affected by the Piz Cengalo, a steep granitic massive located in the central Alps at the border between Switzerland and Italy (see Figure 1), The area was repeatedly affected by large (> 1 Mm^3), rock slope failure processes in the past decades, with the main event on August 23, 2017, being the largest (>3 Mm^3) and most catastrophic reported in recent years, causing 8 fatalities as well as damages in the range of 50M$. A detailed description of the event, its preconditioning factors, potential causes, the dynamics of the rock slope failure and the subsequent debris flow reaching the village of Bondo, is beyond the scope of this work. Thus, the readers are referred to the recent literature for more information on these specific topics (Mergili et al., 2019; Walter et al., 2019).

2 Materials and Methods

We consider Piz Cengalo as an exemplary case to demonstrate the potential of the combination of seismic and spaceborne radar data to provide quantitative information on landslide occurrence in an alpine scenario. We benefit from the high spatial density of the AlpArray seismic network (Hetényi et al., 2018) and from the unprecedented spatial and temporal resolution of Sentinel-1 Synthetic Aperture Radar (SAR) imagery (Torres et al., 2012). In the following, we describe the steps to initially define a candidate location region with seismic data, and then apply change detection investigations on Sentinel-1 SAR imagery to refine the location and identify the slope failure event. Hereafter, we will use the term “landquake” to define “landslide events recorded by seismic sensors”, as increasingly proposed in literature (Chen et al., 2013).

2.1 Seismic data processing

We consider a total of six events occurred at Piz Cengalo between August 21 and October 10, 2017 (see Table 1). The landquakes are characterized by different magnitude in terms of volumes and runout, and occurred all in the same slope but different stages of the progressive failure process: LQ1 occurred two days before the main failure, three events on August 23, 2017, , (LQ2-LQ4), while LQ5 about a month later and LQ6 about two months later). Figure 2 shows the distribution of the AlpArray stations and examples of the signals for the LQ2 detected at different distances from the source. The apparent velocities are on the order of 3 km/s, thus compatible with surface waves generated by surficial mass movements (e.g., Dammeier et al., 2011).

The Swiss Seismological Service (SED) routinely recognizes landslide phenomena in seismic records of stations located in Switzerland and in the vicinity of the national borders. Despite monitoring procedures are not optimized to detect mass movements, these are systematically reported. After an event detection (at least 3 stations triggered on the SED network), a first order manual solution is obtained by identifying coherent energy at multiple stations, identifying these typically as S-waves, by using a regional 3D velocity model. In general, locations are more accurate when seismic stations are close to the event and there is good azimuthal distribution of observations. For the Piz Cengalo landquake event associated to the largest failure (LQ2), the closest station is at ~25km and the location accuracy has uncertainties on the order of ±5 km.

To perform our back analysis on the Piz Cengalo sequence, we define a temporal window of 10 minutes centered on the date and time provided by SED with the manual procedure described above. We consider the waveforms recorded by all the AlpArray broadband stations available for each event and focused on the HHZ channel (i.e., the vertical velocity component of high broad band sampled at or above 80Hz, generally 100 or 200 Hz). The choice of the HHZ channel is justified by previous studies showing that such component usually entails the largest energy in case of landquakes (e.g., Dammeier et al., 2011). We apply a STA/LTA detection (see details and parameters in the Supporting Information, table S1) to find the onset time of the event at each station. Then, we compute the time delay between the first triggered station, assumed to be the closest to the event, and all the other stations identifying an event in the same temporal window. The resulting values are interpolated on a regular grid of 0.25 x 0.25 degrees, spatially smoothed with an average filter (3x3 kernel), and then normalized to obtain a new function defined here as "Likelihood of Landquake Location" (LLL). The candidate region of interest (ROI) potentially affected by a landquake is defined by considering LLL>0.95, and to target the change detection processing on a spatial subset of available Sentinel-1 radar scenes.

2.2 Sentinel-1 SAR data processing

We adopt the change detection processing proposed in (Mondini, 2017), here specifically modified to tackle single events instead of populations of landslides. The analysis is performed to identify potential variations of surface backscattering occurred between the pre- and post-event images, over the area with LLL>0.95 (projected into SAR coordinates). After data acquisition, pre-processing of the radar imagery includes radiometric, and geometric corrections, multi-looking, and filtering of the intensity values to obtain the radar brightness coefficient (Beta Nought, β_0) with a cell resolution of about 14 m x 14 m. Changes of β_0 have demonstrated to be a suitable indicator for the detection of landslide events of different size and occurred in different geographic scenarios (Mondini et al., 2019). In the maps of β_0, changes, landslides appear as clusters of similar values in a bulk of speckles. The β_0 changes map is then segmented using a parametric watershed approach (Roerdink & Meijster, 2000) in which the scale level and the moving window kernel size parameters of the intensity algorithm are automatically assigned minimizing a cost function (Mondini, 2017). The segmentation process is aimed at identifing in the candidate area LLL>0.95 a unique segment (i.e., the largest, potentially delineating changes associated to the landquake) and a number of small segments intercepting the speckle-like effect present in the β_0 changes map. Thus, the landquake is recognized as an outlier in the segment's distribution of the areas. The boundaries of the outlier segment, re-projected from SAR to ground coordinates, provide the potential location of the landquake.

3 Results

Figure 3 shows the exemplary results obtained by analyzing the seismic data available for the LQ2 event. This is the largest landquake, and its seismic signature was detected by tens of stations up to ~500 km distance from the source. The computed LLL function is approximately centered on Piz Cengalo massive. The area within LLL>0.95 is in the order of 10,000 km^2, i.e. ~1% of the entire seismic network considered (the AlpArray covers ~1 Million km^2). However, this is still very large for an accurate identification of a slope failure event affecting an area of about 1 km^2 (Walter et al., 2019).

The initial candidate region defined by the LLL function is used to first identify the available Sentinel-1 imagery in terms of time of acquisition and orbit. In this specific case, the suitable Sentinel-1 orbits are the T015, ascending, and T066, descending, respectively. Then, the change detection processing is not applied to the entire image, but only to the area with LLL>0.95, which is 20% of the acquired SAR scene. Figure 4 shows the best results of the change detection analysis obtained on the ascending T015 imagery (see Supporting Information, Table S2). Due to the temporal proximity of the LQ1-LQ4 sequence (occurred within two days, see Table 1), the LQ2 event cannot be singularly discriminated, because the Sentinel-1 constellation revisit time is of six days. The LQ2, however, has been certainly the main cause of the surface changes, and for this reason we refer hereafter mainly to this event. The outlier segment that identified covers an area of ~0.9 km^2, about two orders of magnitude larger than the average areas of the segment's distribution. The footprint and the dimensions of this segment are in very good agreement with the area affected by the rock avalanche (Walter et al., 2019). The events LQ5 and LQ6 are smaller in magnitude, and the changes on the SAR image cannot be univocally defined as for the LQ2 (see Supporting Information, Figure S2 and S3). Nevertheless, the location of the largest segments identified within the Bondasca valley fall very near to the area affected by the Piz Cengalo landquake sequence.

4 Discussion and Conclusions

Seismic data are capable to provide an indirect evidence of the time of landslide occurrence also in inaccessible locations, but independent validation is necessary for event confirmation and classification (Ekström & Stark, 2013). On the other hand, remote sensing data can deliver direct evidence of the areas hit by landslide events, but independent observations are necessary to identify the exact time of occurrence (Guzzetti et al., 2012). We propose an approach exploiting seismic and remote sensing (specifically, space borne SAR data), which is suitable for the development of automatic pipelines aimed at a systematic identification, location and first evaluation of landslides. We have shown as an exemplary case the application to a sequence of events recently occurred in the Swiss Alps. Our results provide several hints on the potential application of this approach in operational scenarios.

We have applied a STA/LTA approach for the identification of the event on a arbitrary constrained temporal window. The STA/LTA method has shown to be suitable for the automatic detection of mass movements in continuous seismic records also for early warning purposes, although specific calibration of the parameters used is necessary and depend on the sensors, the network configuration, and local conditions (Coviello et al., 2019). One of the main argument against the use of the STA/LTA approach in the detection of mass movent signals lies in the inaccuracy for the determination of the event's onset, which might cause errors on the subsequent location procedures (Fuchs et al., 2018). Since we refine the location using the remote sensing imagery, the STA/LTA approach is sufficient to initially constrain the candidate region for the change detection task. Inaccuracies up to seconds of the STA/LTA detection that would cause dramatic inaccuracies in location routines based on seismic data only, would cause only negligible changes on the LLL function. Despite the candidate location is identified with a basic proximity approach, the source region is already reasonably well constrained for all six LQ events considered (see also Supporting Information, Figure S1). This result is possible only when a relatively high spatial density of seismic sensors is available, such as the AlpArray network. More advanced location routines can be applied, but homogenization of procedures across large areas like entire alpine chain is not straightforward. In addition, an increased level of complexity would not correspond to an obvious increase of accuracies for landslide location.

Another important issue after detection is the distinction and/or classification of the signals recorded in continuous seismic waveforms (e.g., earthquakes, explosion, mass movements, anthropic sources, etc.). Several authors proposed empirical based relationships, signal processing and/or or machine learning strategies, achieving good performances (Dammeier et al., 2016; Hibert et al., 2019; Moore et al., 2017). Here we considered the method proposed in (Manconi et al., 2016) based on the ratio between the local magnitude and the duration magnitude, to distinguish between local earthquakes and landquakes. The results show that with this approach the Piz Cengalo sequence could have been automatically classified as landquakes (see Table 1). This strategy, including the empirical evaluation of the rockslide volumes based on the empirical relationship observed with the duration magnitude, has been recently implemented in an operational regional system in Taiwan showing encouraging results (Chang et al., 2020).

As far as the change detection analysis on the Sentinel-1 SAR data is concerned, the location of landquakes as the LQ2 (i.e. in this case the LQ1-LQ4 sequence) is straightforward. The event is large and causes a relevant drop of the backscattering coefficient in the post event image, spatially over sizing the surrounding random changes always present in SAR images (speckling-like effect). Furthermore, other environmental changes in the area are not relevant, and in this specific case, mostly in the direction of an increase of the backscattering coefficient. The results of the segmentation are unambiguous in all the images whatever the acquisition mode and the polarization are, even if the final segments can be slightly different. Additionally, post processing, like smoothing or gap-filling filtering, can also change partially the final shape of the segment and the identified area. On the contrary, the identification of the LQ5 and LQ6 events shows more complexity and it is not nonambiguous. According to seismic data, their sizes are smaller compared to LQ2, and then correspondingchanges of the backscattering coefficient are expected to be less prominent in the bulk of random speckles. When the signs left on the SAR image amplitude have a size comparable the speckling-like segments, landslides cannot be univocally recognized. Regarding LQ5, the entire area of investigation is also affected by distributed environmental changes dropping the backscattering coefficient, which can be affected by snow and.or other atmospheric disturbances. Only a supervised post processing (further filtering) over the valley, which facilitated the segmentation, allowed to highlight a potential cluster of interest. For LQ6, a small but clear signal is present in the catchment, along the slope, but is not the largest in size considering the entire distribution of segments. There are other signals present in the neighboring valleys that could mislead the analysis. For LQ5 and LQ6, the signals emerge only in the ascending imagery with VH polarization, another possible indication of the change of roughness along the slope(Sung & Holzer, 1976). A potential adaption for the operational implementation of our approach could be running the change detection task on progressively increasing LLL thresholds (e.g., 0.95, 0.975, etc.). This could provide additional hints on possible hot-spots, which can be verified with subsequent SAR acquisitions and/or supplementary remote sensing imagery (space-borne or air-borne).

The key message of this study is to show how the systematic combination of seismic and remote sensig data can be useful for identification and mapping of landslide events. The use of Sentinel-1 SAR satellites shows the advantages of all weather, day and night, and systematic acquisitions at global scale. When available, optical imagery and/or SAR imagery acquired with different bands, full polarimetric, or with higher spatial resolution can eventually contribute to an increase the quality and the quantity of the information.

We conclude remarking that our approach is not intended to be used for early recognition of landslides or as early warning tool. The main goal of an operational implementation could be to systematically populate landslide catalogues relying on quantitative and accurate information on timing, magnitude, and frequency also in remote areas. Improved catalogue completeness is very important for the calibration of regional early warning systems based on rainfall thresholds, as well as on regional hazard assessments(Guzzetti et al., 2019). The availability of remote sensing imagery with daily or sub-daily revisit times could lead to an employment in early detection of landslide events and possibly also in disaster response scenarios, but these potential applications have to be evaluated in future studies.

Acknowledgments

The AlpArray working group (update 23 january, 2021) is listed in the Supporting Information. More information can be found at http://www.alparray.ethz.ch/)

References

Bayer, B., Simoni, A., Mulas, M., Corsini, A., & Schmidt, D. (2018). Deformation responses of slow moving landslides to seasonal rainfall in the Northern Apennines, measured by InSAR. *Geomorphology*, *308*, 293–306. https://doi.org/10.1016/j.geomorph.2018.02.020

Chang, J.-M., Chao, W.-A., Chen, H., Kuo, Y.-T., & Yang, C.-M. (2020). Locating rock slope failures along highways and understanding their physical processes using seismic signals. *Earth Surface Dynamics Discussions*, 1–20. https://doi.org/10.5194/esurf-2020-94

Chao, W.-A., Wu, Y.-M., Zhao, L., Chen, H., Chen, Y.-G., Chang, J.-M., & Lin, C.-M. (2017). A first near real-time seismology-based landquake monitoring system. *Scientific Reports*, *7*. https://doi.org/10.1038/srep43510

Chen, C.-H., Chao, W.-A., Wu, Y.-M., Zhao, L., Chen, Y.-G., Ho, W.-Y., et al. (2013). A seismological study of landquakes using a real-time broad-band seismic network. *Geophysical Journal International*, *194*(2), 885–898. https://doi.org/10.1093/gji/ggt121

Coviello, V., Arattano, M., Comiti, F., Macconi, P., & Marchi, L. (2019). Seismic Characterization of Debris Flows: Insights into Energy Radiation and Implications for Warning. *Journal of Geophysical Research: Earth Surface*, *124*(6), 1440–1463. https://doi.org/10.1029/2018JF004683

Dammeier, F., Moore, J. R., Haslinger, F., & Loew, S. (2011). Characterization of alpine rockslides using statistical analysis of seismic signals. *Journal of Geophysical Research: Earth Surface*, *116*(F4), F04024. https://doi.org/10.1029/2011JF002037

Dammeier, F., Moore, J. R., Hammer, C., Haslinger, F., & Loew, S. (2016). Automatic detection of alpine rockslides in continuous seismic data using Hidden Markov Models. *Journal of Geophysical Research: Earth Surface*, 2015JF003647. https://doi.org/10.1002/2015JF003647

Ekström, G., & Stark, C. P. (2013). Simple scaling of catastrophic landslide dynamics. *Science*, *339*(6126), 1416–1419.

Froude, M. J., & Petley, D. N. (2018). Global fatal landslide occurrence from 2004 to 2016. *Natural Hazards and Earth System Sciences*, *18*(8), 2161–2181. https://doi.org/10.5194/nhess-18-2161-2018

Fuchs, F., Lenhardt, W., Bokelmann, G., & the AlpArray Working Group. (2018). Seismic detection of rockslides at regional scale: examples from the Eastern Alps and feasibility of kurtosis-based event location. *Earth Surface Dynamics*, *6*(4), 955–970. https://doi.org/10.5194/esurf-6-955-2018

Gariano, S. L., & Guzzetti, F. (2016). Landslides in a changing climate. *Earth-Science Reviews*, *162*(Supplement C), 227–252. https://doi.org/10.1016/j.earscirev.2016.08.011

Govi, M., Gullà, G., & Nicoletti, P. G. (2002). Val Pola rock avalanche of July 28, 1987, in Valtellina (Central Italian Alps). In *Reviews in Engineering Geology* (Vol. 15, pp. 71–90). Geological Society of America. https://doi.org/10.1130/REG15-p71

Guzzetti, F., Mondini, A. C., Cardinali, M., Fiorucci, F., Santangelo, M., & Chang, K.-T. (2012). Landslide inventory maps: New tools for an old problem. *Earth-Science Reviews*, *112*(1–2), 42–66. https://doi.org/10.1016/j.earscirev.2012.02.001

Guzzetti, F., Gariano, S. L., Peruccacci, S., Brunetti, M. T., Marchesini, I., Rossi, M., & Melillo, M. (2019). Geographical landslide early warning systems. *Earth-Science Reviews*, 102973. https://doi.org/10.1016/j.earscirev.2019.102973

Hetényi, G., Molinari, I., Clinton, J., Bokelmann, G., Bondár, I., Crawford, W. C., et al. (2018). The AlpArray Seismic Network: A Large-Scale European Experiment to Image the

Alpine Orogen. *Surveys in Geophysics*, *39*(5), 1009–1033. https://doi.org/10.1007/s10712-018-9472-4

Hibert, C., Michéa, D., Provost, F., Malet, J.-P., & Geertsema, M. (2019). Exploration of continuous seismic recordings with a machine learning approach to document 20 yr of landslide activity in Alaska. *Geophysical Journal International*, *219*(2), 1138–1147. https://doi.org/10.1093/gji/ggz354

Huang Mong-Han, Fielding Eric J., Liang Cunren, Milillo Pietro, Bekaert David, Dreger Douglas, & Salzer Jacqueline. (2017). Coseismic deformation and triggered landslides of the 2016 Mw 6.2 Amatrice earthquake in Italy. *Geophysical Research Letters*, *44*(3), 1266–1274. https://doi.org/10.1002/2016GL071687

Lacroix, P., Dehecq, A., & Taipe, E. (2019). Irrigation-triggered landslides in a Peruvian desert caused by modern intensive farming. *Nature Geoscience*, 1–5. https://doi.org/10.1038/s41561-019-0500-x

Manconi, A., Picozzi, M., Coviello, V., De Santis, F., & Elia, L. (2016). Real-time detection, location, and characterization of rockslides using broadband regional seismic networks. *Geophysical Research Letters*, *43*(13), 2016GL069572. https://doi.org/10.1002/2016GL069572

Mergili, M., Jaboyedoff, M., Pullarello, J., & Pudasaini, S. P. (2019). Back-calculation of the 2017 Piz Cengalo-Bondo landslide cascade with r.avaflow. *Natural Hazards and Earth System Sciences Discussions*, 1–30. https://doi.org/10.5194/nhess-2019-204

Mondini, A. C. (2017). Measures of Spatial Autocorrelation Changes in Multitemporal SAR Images for Event Landslides Detection. *Remote Sensing*, *9*(6), 554. https://doi.org/10.3390/rs9060554

Mondini, A. C., Santangelo, M., Rocchetti, M., Rossetto, E., Manconi, A., & Monserrat, O. (2019). Sentinel-1 SAR Amplitude Imagery for Rapid Landslide Detection. *Remote Sensing*, *11*(7), 760. https://doi.org/10.3390/rs11070760

Moore, J. R., Pankow, K. L., Ford, S. R., Koper, K. D., Hale, J. M., Aaron, J., & Larsen, C. F. (2017). Dynamics of the Bingham Canyon rock avalanches (Utah, USA) resolved from topographic, seismic, and infrasound data. *Journal of Geophysical Research: Earth Surface*, 2016JF004036. https://doi.org/10.1002/2016JF004036

Petley, D. N. (2004). The evolution of slope failures: mechanisms of rupture propagation. *Nat. Hazards Earth Syst. Sci.*, *4*(1), 147–152. https://doi.org/10.5194/nhess-4-147-2004

Roerdink, J. B. T. M., & Meijster, A. (2000). The Watershed Transform: Definitions, Algorithms and Parallelization Strategies. *Fundamenta Informaticae*, *41*(1,2), 187–228. https://doi.org/10.3233/FI-2000-411207

Stead, D., & Wolter, A. (2015). A critical review of rock slope failure mechanisms: The importance of structural geology. *Journal of Structural Geology*, *74*, 1–23. https://doi.org/10.1016/j.jsg.2015.02.002

Sung, C. C., & Holzer, J. A. (1976). Scattering of electromagnetic waves from a rough surface. *Applied Physics Letters*, *28*(8), 429–431. https://doi.org/10.1063/1.88809

Tanyaş, H., van Westen, C. J., Allstadt, K. E., Anna Nowicki Jessee, M., Görüm, T., Jibson, R. W., et al. (2017). Presentation and Analysis of a Worldwide Database of Earthquake-Induced Landslide Inventories. *Journal of Geophysical Research: Earth Surface*, *122*(10), 2017JF004236. https://doi.org/10.1002/2017JF004236

Torres, R., Snoeij, P., Geudtner, D., Bibby, D., Davidson, M., Attema, E., et al. (2012). GMES Sentinel-1 mission. *Remote Sensing of Environment*, *120*, 9–24. https://doi.org/10.1016/j.rse.2011.05.028

Walter, F., Amann, F., Kos, A., Kenner, R., Phillips, M., de Preux, A., et al. (2019). Direct observations of a three million cubic meter rock-slope collapse with almost immediate initiation of ensuing debris flows. *Geomorphology*, 106933. https://doi.org/10.1016/j.geomorph.2019.106933

Weichert, D., Horner, R. B., & Evans, S. G. (1994). Seismic signatures of landslides: The 1990 Brenda Mine collapse and the 1965 hope rockslides. *Bulletin of the Seismological Society of America*, *84*(5), 1523–1532.

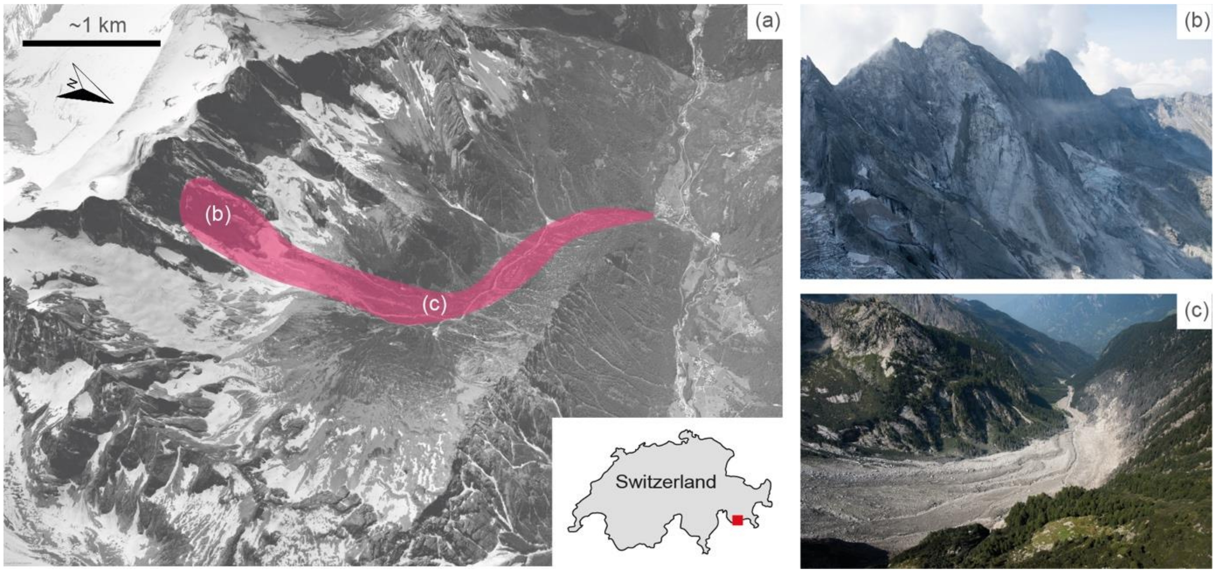

Figure 1. Overview of the area of investigation. (a) Google Earth© view of the Val Bondasca, with approximate outline of the area affected by the Piz Cengalo (46.29475° N, 9.602056° E) rock avalanche and subsequent debris flows; (b) Detail of the release area, August 25, 2017; (c) Detail of the deposits, August 30 2017. © Photos VBS swisstopo Flugdienst.

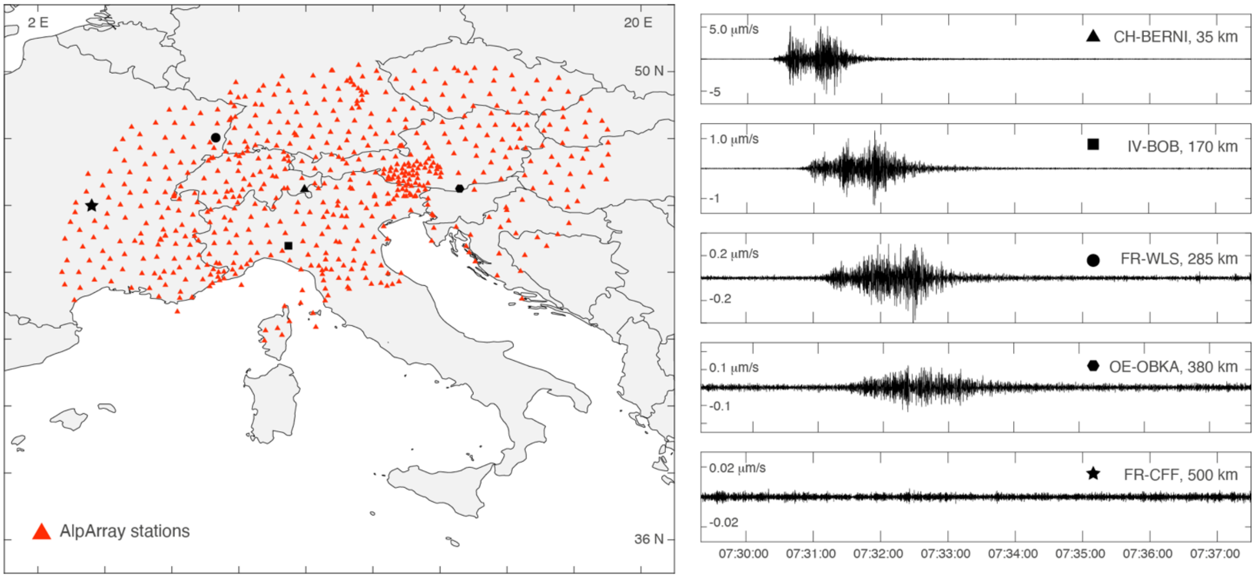

Figure 2. Seismic network and data (left) The AlpArray network of broad band stations. (right) Selected signals (vertical component HHZ) recorded by AlpArray stations located at different distances from event LQ2 (see table 1), occurred on August 23, 2017 (i.e., the main Piz Cengalo rock avalanche event).

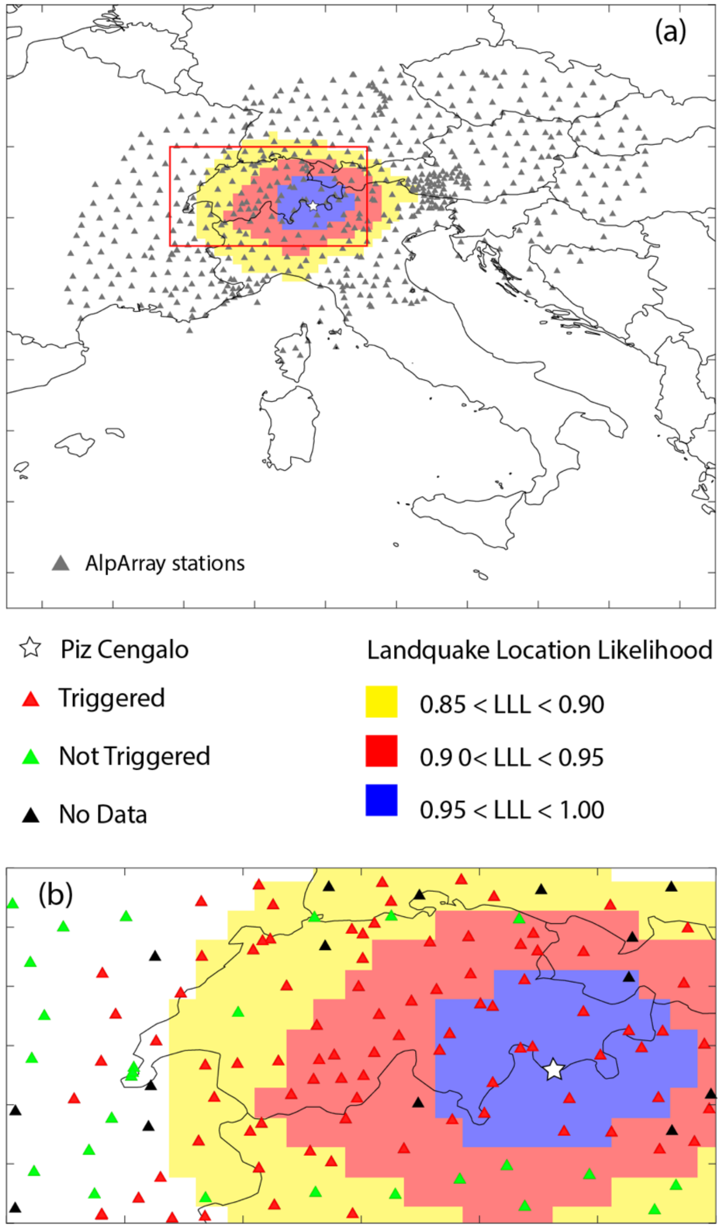

Figure 3. Likelihood of Landquake Location (LLL) based on the arrival time of seismic signals recorded by AlpArray stations. This basic analysis of the seismic data is used to constrain the approximate location where a landslide event has occurred. (a) LLL over the entire AlpArray network (b) Zoom on the areas with high likelihood. The area 0.95<LLL<1.0 is used to confine the change detection analysis. True location of the Piz Cengalo event (white star) is also shown.

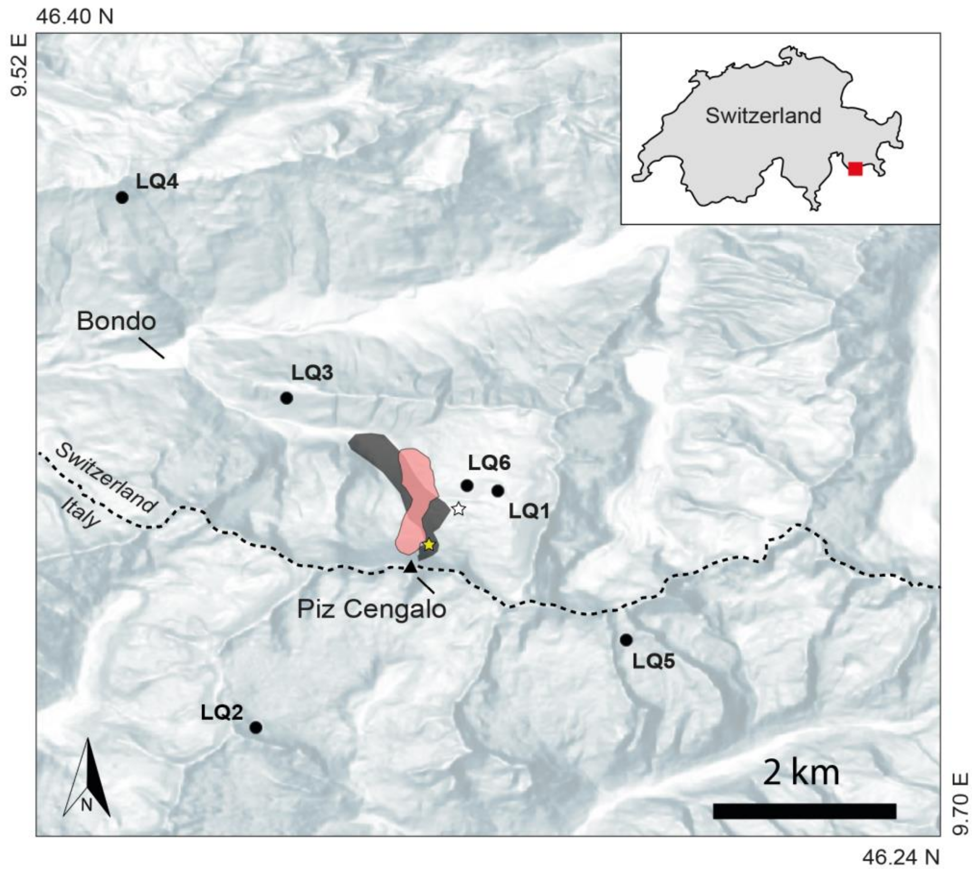

Figure 4. Results of the change detection analysis. The red polygon shows the area identified as potential landquake location for the main Landquake event (i.e., LQ1-LQ4) identified by processing the Sentinel-1 pre- and post-event, while the gray polygon is the area hit by the rock avalanche (cf. Walter et al., 2019). The white star and the yellow star show the locations of the largest segments for LQ5 and LQ6, respectively, identified within the Bondasca valley.The black dots show the epicentral locations provided by SED (see Table 1).

Event ID	Date/Time (UTC)	ML	MD*	ML/MD	Vol (Mm3)
LQ1	2017-08-21T09:29:09	2.3	3.03	0.75	0.078 - 0.167
LQ2	2017-08-23T07:30:27	3.0	3.71	0.80	1.65 - 2.61
LQ3	2017-08-23T09:03:57	1.3	2.86	0.45	0.02 - 0.14
LQ4	2017-08-23T09:36:16	2.1	3.22	0.65	0.12 - 0.50
LQ5	2017-09-15T20:04:36	2.3	3.26	0.70	0.23 - 0.41
LQ6	2017-10-10T02:58:41	1.1	2.65	0.41	0.014 - 0.035

Table 1. Summary of the landquakes analyzed in this study and associated to the Piz Cengalo slope failure. ML are estimated by SED, while average magnitude duration (MD) and volumes are computed following Manconi et al., 2016, by considering the event duration on all triggered AlpArray stations. Note that all LQ events have ML/MD have ML/MD less or equal to 0.8, i.e. they can be discerned from earthquake events which typically have ML/MD ~ 1.